

Communications

Detection and Measurement of Retinal Vessels in Fundus Images Using Amplitude Modified Second-Order Gaussian Filter

Luo Gang, Opas Chutatape*, and Shankar M. Krishnan

Abstract—In this paper, the fitness of estimating vessel profiles with Gaussian function is evaluated and an amplitude-modified second-order Gaussian filter is proposed for the detection and measurement of vessels. Mathematical analysis is given and supported by a simulation and experiments to demonstrate that the vessel width can be measured in linear relationship with the “spreading factor” of the matched filter when the magnitude coefficient of the filter is suitably assigned. The absolute value of vessel diameter can be determined simply by using a precalibrated line, which is typically required since images are always system dependent. The experiment shows that the inclusion of the width measurement in the detection process can improve the performance of matched filter and result in a significant increase in success rate of detection.

Index Terms—Fundus image, matched filter, retinal vessel, vessel measurements.

I. INTRODUCTION

Ocular fundus image can provide information on pathological changes caused by some eye diseases and early signs of certain systemic diseases, such as diabetes and hypertension. Analyzing and interpreting fundus images has become a necessary and important diagnostic procedure in ophthalmology and a considerable research effort has been devoted to automate this process. The structure of retinal vessels is a prominent feature that reveals further information on the state of diseases that are reflected in the form of measurable abnormalities in diameter, color, and tortuosity. Thus, reliable methods of vessel detection that preserve various vessel measurements are needed.

There are two different kinds of detector that have been explored for vessel detection: edge detector and matched filter. The edge-detection method works by detecting the left and right edges of vessel with edge detector, such as Sobel operator [1] and Canny’s method [2], morphological detector [3], gradient operator [4], directional matched low-pass differentiator template [5] and optimized Canny’s detector [6]. Matched filter method works by convolving the vessels with a filter designed according to the suitable model of vessel profile [7]–[12]. Blurred half-elliptical vessel [8], Gaussian vessel [7], [9], [12], and simple rectangular vessel [4], [11] have been proposed. The diameter measurement is based on model estimation, i.e., to find the most matched model for the vessel profile and then determine the vessel diameter according to a specified parameter of the model [8], [9].

For the vessel tracking, the matched filter helps ignoring small branches at a bifurcation point without any special handling, thus

Manuscript received July 21, 2000; revised June 27, 2001. This work was supported by the School of EEE, Nanyang Technological University under a research grant. Asterisk indicates corresponding author.

L. Gang and S. M. Krishnan are with the School of Electrical and Electronic Engineering, Nanyang Technological University, 639798 Singapore.

*O. Chutatape is with the School of Electrical and Electronic Engineering, Nanyang Technological University, Block S1, Nanyang Avenue, 639798 Singapore (e-mail: eopas@ntu.edu.sg).

Publisher Item Identifier S 0018-9294(02)00646-8.

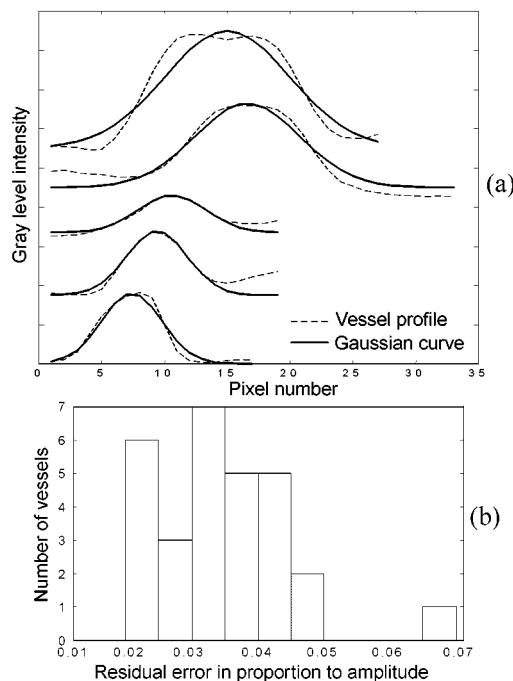


Fig. 1. Estimation of blood vessel profile. (a) Inverted profiles of the cross section of several blood vessels and their fitted Gaussian curves. (b) Histogram of mean residual absolute error of fitting.

allowing the tracking process to follow one major branch continuously [9]. Hence the matched filter is chosen for the vessel detection in this research.

Although the center point of vessel can be detected with matched filter, the diameter measurement is not simple. As reported in [7], the vessels of varying widths could be located with one filter. Vice versa, a vessel segment can be detected with the filters of varying widths, as demonstrated in the following sections, but it was noticed that the values of convolution peaks were different according to different filter widths and the vessel diameter cannot be obtained from the readily available convolution results in the process of location detection. This paper reveals the possibility to measure the vessel diameter with matched filter and its influence on the vessel extraction.

II. SECOND-ORDER GAUSSIAN FILTER FOR VESSEL DETECTION

A. Validation of Modeling Vessels in Color Fundus Image

An exact model of vessel image is difficult to describe since it is associated with many factors, such as the tissue’s characteristics, light source and the modulation transfer function of the imaging system that depend on both the optical and electronic elements. It is clearly not easy to obtain all specifications of the whole system to figure out the exact model of a vessel and neither is it necessary. An approximation that conforms to the statistical features and fulfills a specific application should be acceptable and sufficient.

In this paper, the Gaussian function model for vessel profile as described in [7] was further studied. Here, the vessel detection is based on the green component of color fundus image since blood vessels have high contrast on it. A few samples of vessel profile sections are shown

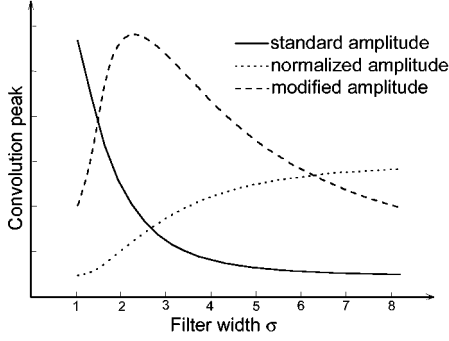


Fig. 2. Values of convolution peaks obtained with standard, normalized, and modified amplitude second-order Gaussian filters in the detection of a retinal blood vessel. The filters are described in (2), (3), and (4), respectively.

in Fig. 1(a) as well as the fitted Gaussian curves with least square errors criteria. For the purpose of simplicity, the profiles of vessel section and fitting curves are inverted. The Gaussian function used for fitting is

$$g(x) = Ae^{-(x-z)^2/2w^2} \quad (1)$$

where x is the horizontal coordinate, A is the amplitude of the profile, z is the position of profile peak, and w is a specific parameter of Gaussian function that controls the width of profile. The mean absolute residual errors of fitting are less than four gray levels. The formula for calculating the error is $\{\sum |(m_i - v_i)|\}/n$, where m_i and v_i are profile values of the model and actual data, respectively, and n is the number of pixels on the cross-section profile of vessel. In proportion to the amplitude of Gaussian curve, the relative error ranges from 2% to 5%, averaging at 3.4% [Fig. 1(b)]. It can be observed that the residual errors are mainly at the periphery. The background contributes less to the convolution response if a zero-mean, second-order differential Gaussian filter is adopted. These observations suggest that modeling a vessel profile with Gaussian curve is an appropriate approach.

B. Amplitude-Modified Second-Order Gaussian Filter

The second-order differential Gaussian filter of zero-mean for vessel detection is described by

$$f(x) = \frac{1}{\sqrt{2\pi}\sigma^5} (x^2 - \sigma^2) e^{-x^2/2\sigma^2} \quad (2)$$

where σ is a specific parameter of the Gaussian filter function that controls the width of filter, like the w in (1). The possibility of using this type of filter for measurement of vessel width is discussed in this paper. Fig. 2 shows the relationship between the value of convolution peak and filter width for an arbitrary vessel. The solid curve corresponds to standard filters described in (2), from which it can be noticed that the wider the filter, the smaller the convolution peak. Therefore, it is not easy to determine the vessel width with this kind of filter. To eliminate the amplitude factor in the standard second-order Gaussian function, the filter is revised as

$$f(x) = (x^2 - \sigma^2) e^{-x^2/2\sigma^2} \quad (3)$$

and the results were shown as dot line in Fig. 2. Contrary to the standard filter, here the wider the filter, the higher the convolution peaks. However, it still is not possible to determine the vessel width. Now if the amplitude factor is further modified to a moderate value as follows, i.e., the power of σ in the amplitude denominator is changed to three

$$f(x) = \frac{1}{\sqrt{2\pi}\sigma^3} (x^2 - \sigma^2) e^{-x^2/2\sigma^2} \quad (4)$$

The dashed line in Fig. 2 shows the results of this modified second-order Gaussian filter. A peak is seen to emerge, which indicates that such a filter can give the highest response for a specific vessel. Consequently, it is possible to measure the vessel width with a modified Gaussian filter.

The convolution hits the maximum when the two peaks of the Gaussian vessel and the Gaussian filter coincide. The convolution peak equals

$$h(t) = \int_{-\infty}^{+\infty} \frac{1}{\sqrt{2\pi}\sigma^t} (x^2 - \sigma^2) e^{-(x^2/2)((w^2 + \sigma^2)/w^2\sigma^2)} dx \quad (5)$$

where the power of σ in amplitude factor of second-order Gaussian filter is set to parameter t and the amplitude of vessel profile is assumed to be 1 for simplification. Replacing the exponential order term $(w^2 + \sigma^2)/(w^2\sigma^2)$ with $1/s^2$ and rearranging (5) will give

$$h(t) = \frac{1}{\sqrt{2\pi}\sigma^t} \int_{-\infty}^{+\infty} \left((x^2 - s^2) e^{-x^2/2s^2} + (s^2 - \sigma^2) e^{-x^2/2s^2} \right) dx. \quad (6)$$

The first term in the integrand is second-order differential Gaussian function and its integral equals zero. By using the relationship

$$\int_{-\infty}^{+\infty} e^{-x^2} dx = \sqrt{\pi} \quad (7)$$

(6) becomes

$$\frac{1}{\sqrt{2\pi}\sigma^t} \cdot \sqrt{2\pi} (s^2 - \sigma^2) s = \frac{w\sigma^{5-t}}{(w^2 + \sigma^2)^{1.5}}. \quad (8)$$

The preceding equation gives the convolution peak value of a vessel associated with parameter w and a second-order Gaussian filter associated with parameter σ . When parameter t changes, the value in the preceding equation will change accordingly. The case of particular interest is when $t = 3.5$ which will give

$$h = \frac{w\sigma^{1.5}}{(w^2 + \sigma^2)^{1.5}}. \quad (9)$$

It can be easily derived that the convolution peak hits maximum when $\sigma = w$. The conditions of maximum values for other cases can also be derived, e.g., when $t = 5.0, 4.0, 3.0$, or 2.0 , the conditions are $\sigma = 0$, $\sigma = 0.707w$, $\sigma = 1.414w$, and $\sigma^2 = \sigma^2 + w^2$, respectively.

According to the results derived above, for the detection of Gaussian vessel with parameter w , the matched filter with parameter $\sigma = w$ gives the maximum convolution peak if a second-order Gaussian filter of parameter $t = 3.5$ is used. Similarly, if the second-order Gaussian filters of parameter $t = 4$ and $t = 3$ are used, the filters associated with $\sigma = 0.707w$ and $\sigma = 1.414w$ give the respective maximum convolution peaks. However, for the cases of parameter $t = 5$ and $t = 2$, there is no such a relationship between the filter width and the vessel width.

III. SIMULATION AND EXPERIMENT

A. Simulation of Vessel Measurement

Simulation of vessel detection using the second-order Gaussian filter with different values of parameter t was performed and the results are shown in Fig. 3. Given a value of parameter t , a total of 20 vessel profiles of Gaussian model whose parameter w ranging from one to 20 pixels were generated and 30 second-order Gaussian filters whose parameter σ ranging from 1 to 30 pixels were used to convolve with every vessel. The maximum peak was obtained by interpolating with all the 30 convolution peaks of implemented filters. It can be observed that the

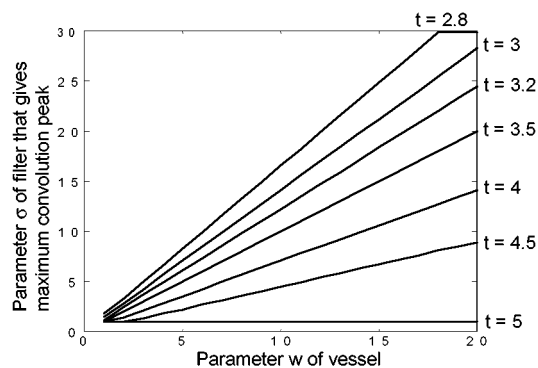


Fig. 3. Filter widths against vessel widths for different parameter t .

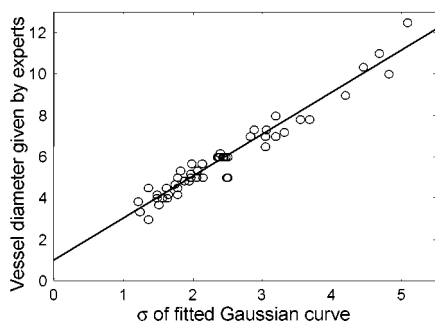


Fig. 4. Linear relationship between parameter σ of fitted Gaussian curve and the diameter of blood vessel.

simulation results with parameter t at 3.0, 3.5, 4.0 support the mathematical analysis above. For parameter t at other arbitrary values within 2–5, such as 2.8, 3.2, or 4.5, the parameter σ that gives the maximum convolution peak is also linearly related to the parameter w of vessel. The difference is only the slope, which is larger for smaller value of t . Therefore, a vessel can be enclosed and measured with fewer filters when a larger parameter t is adopted, but the precision is lower. A more attractive case is when parameter t equals 3.5. The parameter w of a vessel equals the parameter σ of the filter when the maximum convolution peak occurs. This makes the filter with $t = 3.5$ optimal for vessel detection and measurement.

B. Measurement of Vessel Diameter

It is impossible to define the exact width of vessel image modeled as a Gaussian curve because it is endlessly continuous. In [9], a value of 1.96σ was defined as the half width of vessel based on the fact that the integration within $\pm 1.96\sigma$ reaches 95% of the integration of the whole domain. In [13] and [14], vessel diameters were defined as the distance between the points of 50% intensity change of the vessel profile. However, there is little evidence to suggest that the vessel edges are really located at these points.

A definition of vessel width based on a calibration procedure is presented here. It is found that the specified parameter of Gaussian function, σ , is linearly related to the vessel width measured by visual inspection of the digital image in the experiment, as shown in Fig. 4. A total 50 profiles of various vessels were extracted from color fundus images. The diameters of these vessels were estimated by five experts based on visual inspection and the average of their measurements were used for analysis. The σ value of each profile was obtained using the above amplitude-modified Gaussian filter with $t = 3.5$. Although random errors exist in the direct measurement, the linear relationship is indicated in a reasonable limit and the slope will be more accurate if sufficient

data are provided. Only the offset of the fitted line may not be accurate because the calibration is just based on a visual observation. It may contain a constant error depending on the calibration procedure. However, this constant measurement error can be easily corrected if a standard object is given. Thus the relationship between the parameter σ and the actual diameter of vessel for a specified imaging system can be determined. Given the fitted straight line in Fig. 4, the relationship is $d = 2.03\sigma + 0.99$ where d is the diameter of a vessel.

Determination of exact position of vessel edge from mathematical models has caused some different definitions and the issue is further complicated by the fact that the models are even different for different images such as X-ray angiogram, fluorescein image and color image. The objective definition of vessel width used in this paper can be associated with a precise calibration without any consideration of vessel edge. This not only simplifies the problem, but also enables various measuring results of vessel width to be comparable and exchangeable among different assessors.

C. Implementation and Experiment on Vessel Detection

In order to suppress error in the vessel detection, the filter was designed to be two-dimensional for matching vessel segment instead of matching a single profile of vessel cross section, hence, it is described as

$$f(x, y) = \frac{1}{\sqrt{2\pi}\sigma^{3.5}} (x^2 - \sigma^2) e^{-x^2/2\sigma^2}$$

when

$$y \leq L, \quad |x - c| \leq \frac{FW}{2} \quad (10)$$

where L is the length of filter window, c is the x position of the center line of filter window along y axis, and FW is the width of filter window. Here, the orientation of filter is assumed to be aligned along the y axis. During the vessel tracking, the filter is rotated accordingly. The output of this filter hits its peak only if its orientation is aligned with that of vessel. Thus, the location and orientation of vessel segment can be detected.

The size of filter window is adaptively adjusted according to the vessel width in the detection by keeping the filter size proportional to σ , i.e., the standard filter model enlarges or shrinks linearly to match the vessels. This is helpful to build a sufficiently large filter to cover wide vessels and build an appropriately small filter to avoid extra pattern when detecting thin vessels. Since many of lesions occur around capillary and many of thin vessels are irregularly tortuous, a large filter probably gives a wrong response due to too many extra patterns that it covers. The threshold is also adjusted in accordance with predicted vessel width. As mentioned above, the maximum convolution peak in the one-dimensional case is given by (9) when $w = \sigma$ and $t = 3.5$, that is

$$\frac{\sigma^{2.5}}{(2\sigma^2)^{1.5}} = \frac{1}{2\sqrt{2}\sigma}. \quad (11)$$

Hence, the threshold used in the detection is $R/(L\sqrt{\sigma})$, where R is a constant that is associated with the expected minimum contrast of vessel and L , the length of filter window, is for normalization, i.e., eliminating its influence on the value of convolution peak.

From (9) and (11), one can see that the measurement of vessel width is crucial to correct thresholding in the detection because the value of convolution peak varies with σ . It may lead to a wrong thresholding if the vessel width is not measured correctly. An example is given as shown in Fig. 5. In Fig. 5(b), the filter width is fixed during the detection. A wide filter gives a high response to a wide vessel (matched) and a low response to a thin vessel (nonmatched). Therefore, a threshold

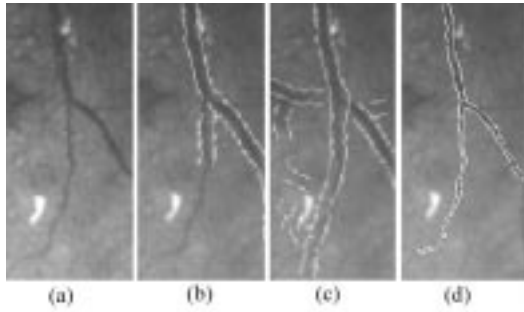


Fig. 5. Thresholding in blood vessel detection with fixed and adaptive filter width. (a) original image, (b) fixed filter width and strict threshold, (c) fixed filter width and loose threshold, and (d) adaptive filter width and adaptive threshold.

suitable for the wide vessel is not suitable for the thin vessel. If the threshold is tight, then some thin vessels cannot be detected. If the threshold is loose some false vessels may emerge as shown in Fig. 5(c). Fig. 5(d) shows the detection using adaptive filter width, which identifies the thin vessel without false outcome of wide vessel.

To avoid a wrong threshold caused by an occasional false measurement, the continuity of diameter measurement is verified. If it varies irregularly then the estimation is considered false and will be ignored without modifying the threshold.

Fig. 6 shows an experimental result of vessel detection with a second-order Gaussian filter of parameter $t = 3.5$. The image shown in Fig. 6(a) is the green component of a color fundus image with conspicuous exudates. The vessel-detection pattern is shown in Fig. 6(b) in which two circles indicate the locations of the optic disk and fovea. It can be seen that vessels were successfully detected except a segment indicated by a black arrow, where an error occurs due to a hemorrhage attaching to the blood vessel. The diameters of all vessels as measured by the proposed filter, however, show good agreement with visual inspection.

To evaluate the proposed method and test the benefit of vessel width measurement to vessel detection, a total of 1873 vessels that are longer than $1/2$ disc diameter in 48 color fundus images were fed to the algorithms with and without width measurement. Except for the additional vessel width measurement and then changing matched filter and threshold accordingly in the proposed method, the program sequences of two algorithms are the same. The images include 36 scanned images of color slide films and 12 charge-coupled device images obtained from digital retinal camera. Manifest lesions, e.g., hemorrhages and exudates can be found around vessels in 27 of these images. The experimental results are shown in Table I.

A successful detection is defined as a tracking of vessel without leaving out any obvious segment. A partly successful detection must acquire more than half of a vessel path; otherwise, it is categorized as failed detection. An erroneous detection means that a part of the detection result of a vessel is actually not blood vessel.

Among the partly successful detections, more than 90% is due to weak pattern of capillaries, the others are caused by lesions or two vessels that are so close that the weaker one is ignored in the scanning procedure. All the failed detections occurred due to very weak pattern of capillaries. As for the erroneous detections, more than 73% is from the effect of lesions, e.g., the case indicated in Fig. 6(b) and the others are due to normal pattern of nonvessels, e.g., the case in Fig. 5(c).

From the experimental results it can be seen that for blood vessel detection the major cause for missing vessel is the weakness of capillary pattern and the detection error is mainly caused by the lesions. Basically 94.3% of blood vessels can be detected by the proposed method. With measurement of vessel width, the rate of successful detection is significantly improved because the matched filter and threshold can be



Fig. 6. An application of second-order Gaussian filter for retinal vessel detection. (a) Green component of color fundus image. (b) Detecting and quantifying results.

TABLE I
EXPERIMENTAL RESULTS FROM THE DETECTION OF 1873 VESSELS IN 48
COLOR FUNDUS IMAGES

	Algorithm using width measurement	Algorithm not using width measurement
Successful rate	85.5%	61.4%
Partly successful rate	8.8% (91.4% lesion related)	18.1% (93.2% lesion related)
Failure rate	3.2%	13.1%
Error rate	2.5% (83.7% lesion related)	7.4% (73.4% lesion related)

optimized to adapt to both wide and thin vessels. The results in Table I suggest that the vessel width should be measured and taken into account to build the true matched filter.

IV. CONCLUSION

In this paper, it is shown that the Gaussian curve is suitable for modeling the intensity profile of the cross section of retinal vessels in color fundus images. Based on this elaboration, the amplitude-modified second-order Gaussian filter for retinal vessel detection is proposed and its performance is demonstrated. The mathematical analysis, vessel-detection simulation and its assessment on various fundus images show that the Gaussian filter with modified amplitude can be effectively used

to detect and measure the retinal vessels. The vessel width measurement not only provides the size of blood vessel but it is also useful for optimizing the matched filter to improve the successful rate of detection.

ACKNOWLEDGMENT

The authors would like to thank the Singapore National Eye Center for providing image data and clinical details.

REFERENCES

- [1] W. Pratt, *Digital Image Processing*. New York: Wiley, 1978.
- [2] J. F. Canny, "A computational approach to edge detection," *IEEE Trans. Pattern Anal. Machine Intell.*, vol. PAMI-8, pp. 679–698, 1986.
- [3] Y. Qian, S. Eiho, N. Sugimoto, and M. Fujita, "Automatic extraction of coronary artery tree on coronary angiograms by morphological operators," *Comput. Cardiol.*, vol. 25, p. 765, 1998.
- [4] Y. Sun, "Automated identification of vessel contours in coronary arteriogram by an adaptive tracking algorithm," *IEEE Trans. Med. Imag.*, vol. 8, pp. 78–88, Feb. 1989.
- [5] Can, H. Shen, J. Turner, H. Tanenbaum, and B. Roysam, "Rapid automated tracing and feature extraction from retinal fundus images using direct exploratory algorithms," *IEEE Trans. Inform. Technol. Biomed.*, vol. 3, pp. 125–138, June 1999.
- [6] P. M. J. Zwet, M. Nettesheim, J. Gerbrands, and J. Reiber, "Derivation of optimal filters for the detection of coronary arteries," *IEEE Trans. Med. Imag.*, vol. 17, pp. 108–120, Feb. 1998.
- [7] S. Chaudhuri, S. Chatterjee, N. Katz, and M. Goldbaum, "Detection of blood vessels in retinal images using two-dimensional matched filters," *IEEE Trans. Med. Imag.*, vol. 3, pp. 263–269, Sept. 1989.
- [8] F. P. Miles and A. L. Nuttall, "Matched filter estimation of serial blood vessel diameters from video images," *IEEE Trans. Med. Imag.*, vol. 12, pp. 147–152, June 1993.
- [9] L. Zhou, M. S. Rzeszotarski, L. J. Singerman, and J. M. Chokreff, "The detection and quantification of retinopathy using digital angiogram," *IEEE Trans. Med. Imag.*, vol. 13, pp. 619–626, Aug. 1994.
- [10] O. Chutatape, L. Zheng, and S. M. Krishnan, "Retinal blood vessel detection and tracking by matched Gaussian and Kalman filters," in *Proc. 20th Annu Conf. IEEE Engineering in Medicine and Biology Society*, 1998, pp. 3144–3149.
- [11] W. J. Ohley, Y. Sun, A. S. Most, and D. O. Williams, "A computationally efficient algorithm for tracking coronary arteries on digital arteriograms," in *Proc. IEEE 11th Northeast Bioengineering Conf.*, Worcester, MA, 1985, pp. 255–258.
- [12] A. Hoover, V. Kouznetsova, and M. Goldbaum, "Locating blood vessels in retinal images by piecewise threshold probing of a matched filter response," *IEEE Trans. Med. Imag.*, vol. 19, no. 3, pp. 203–210, 2000.
- [13] V. Patel, "A new concept in accurately measuring retinal vessel diameter from transmittance and densitometry profile of fundus photographs," *ARVO Abstract. Invest. Ophtha. Vis. Sci.*, vol. 33, no. 4, pp. 804–804, 1992.
- [14] P. Jensen, "Video photography of human retinal vessel diameter *in vivo*," *ARVO Abstract. Invest. Ophtha. Vis. Sci.*, vol. 33, no. 4, p. 1048, 1992.

An Advanced Detrending Method With Application to HRV Analysis

Mika P. Tarvainen, Perttu O. Ranta-aho, and Pasi A. Karjalainen

Abstract—An advanced, simple to use, detrending method to be used before heart rate variability analysis (HRV) is presented. The method is based on smoothness priors approach and operates like a time-varying finite-impulse response high-pass filter. The effect of the detrending on time- and frequency-domain analysis of HRV is studied.

Index Terms—Heart rate variability, signal detrending, smoothness priors, spectral analysis.

I. INTRODUCTION

Heart rate variability (HRV) is a widely used quantitative marker of autonomic nervous system activity. Various time- and frequency-domain methods have been applied to HRV analysis [1]. A traditional spectral method, power spectral density (PSD) estimation, provides information about power distribution as a function of frequency. Spectral estimation inherently assumes that the signal is at least weakly stationary. However, real HRV is usually nonstationary. Nonstationarities like slow linear or more complex trends in the HRV signal, can cause distortion to time- and frequency-domain analysis. Origins for nonstationarities in HRV are discussed, e.g., in [2].

Two kinds of methods have been used to get around the nonstationarity problem. Weber *et al.* [3] suggested that HRV data should be systematically tested for nonstationarities and that only stationary segments should be analyzed. Representativeness of these segments in some cases, in comparison with the whole HRV signal, was, however, questioned in [4]. Other methods try to remove the slow nonstationary trends from the HRV signal before analysis. The detrending is usually based on first-order [5], [6] or higher order polynomial [6], [7] models.

In this paper, we present an advanced detrending procedure based on smoothness priors approach. The presented method is simple to use, since the frequency response can be adjusted adequately to different situations by a single parameter. The properties of the method are tested by applying it to real RR interval data and the effect of the method on time- and frequency-domain analysis of HRV is considered.

II. METHODS

A. Data Acquisition

The Electrocardiogram (ECG) was recorded continuously (NeuroScan by NeuroSoft Inc.) during a passive event related potential paradigm, where subject sat in a chair while auditory pitch stimuli were delivered to right ear. Sampling rate of the ECG was 500 Hz. Discrete event series, $R_i - R_{i-1}$ intervals as a function of R_i occurrence times, was constructed by an adaptive QRS detector algorithm. The QRS detector was based on the one presented in [8]. As a result of the detection algorithm, an unevenly sampled RR interval time series was obtained. In order to recover an evenly sampled signal from the irregularly sampled event series, cubic interpolation was applied.

Manuscript received March 2, 2001; revised September 28, 2001. *Asterisk indicates corresponding author.*

*M. P. Tarvainen is with the University of Kuopio, Department of Applied Physics, P.O. Box 1627, FIN-70211 Kuopio, Finland (e-mail: Mika.Tarvainen@uku.fi).

P. O. Ranta-aho and P. A. Karjalainen are with the University of Kuopio, Department of Applied Physics, FIN-70211 Kuopio, Finland.

Publisher Item Identifier S 0018-9294(02)00637-7.